

Original Article

DOI 10.1007/s12206-020-0432-9

Keywords:

- Bending procedure
- Mandibular reconstruction
- Motorized bending apparatus
- Spring-back
- Surgical plate

Correspondence to:

Gunwoo Noh  
gunwoo@knu.ac.kr

Citation:

Park, S.-M., Lee, J., Park, S., Lee, J.-W., Park, M., Kim, Y., Noh, G. (2020). Practical bending-angle calculation for an automated surgical plate bending apparatus. *Journal of Mechanical Science and Technology* 34 (5) (2020) 2101–2109. <http://doi.org/10.1007/s12206-020-0432-9>

Received October 9th, 2019

Revised February 3rd, 2020

Accepted March 4th, 2020

† Recommended by Editor  
Seungjae Min

# Practical bending-angle calculation for an automated surgical plate bending apparatus

Si-Myung Park<sup>1</sup>, Jeonghwan Lee<sup>2</sup>, Seungbin Park<sup>2</sup>, Jung-Woo Lee<sup>3</sup>, Minsoo Park<sup>4</sup>,  
Youngjun Kim<sup>2</sup> and Gunwoo Noh<sup>5</sup>

<sup>1</sup>Center for Medical Robotics, Korea Institute of Science and Technology, Seoul 02792, Korea, <sup>2</sup>Center for Bionics, Korea Institute of Science and Technology, Seoul 02792, Korea, <sup>3</sup>Department of Oral & Maxillofacial Surgery, School of Dentistry, Kyung Hee University, Seoul 02447, Korea, <sup>4</sup>Department of Mechanical System Design Engineering, Seoul National University of Sci. and Tech., Seoul 01811, Korea, <sup>5</sup>School of Mechanical Engineering, Kyungpook National University, Daegu 41566, Korea

**Abstract** Surgical plates used for reconstructive surgery require a repetitive manual bending process to fit the plate to the defect during reconstruction. However, this process may not produce a plate that fits well, and repetitive bending may significantly increase the risk of plate fracture due to the accumulation of residual stress. In this study, the input angle is calculated using a proposed finite element process that considers the spring-back effect and improves the accuracy of the bending results without the need for repetitive bending. Bending tests for two arbitrary target angles (15° and 30°) are performed using the apparatus to demonstrate its effectiveness. Accurately bent plates are obtained from a single bending trial, unlike the use of another input angle that does not consider spring-back. Therefore, the proposed bending procedure could potentially replace the repetitive manual bending process and reduce the residual stress within the plate, thus lowering the risk of plate failure.

## 1. Introduction

Surgical plates are widely used in orthopedic, oral, maxillofacial, plastic, and other forms of reconstructive surgery. During surgery, a plate is generally required to undergo repetitive manual bending in order for it to fit the defect, a process conducted by the surgeon using tools such as a bending press or bending iron. This process typically involves multiple trials to fit the plate to the shape of the surgical area; this repetitive bending not only prolongs the operating time but also reduces the life of the plate [1]. Plate removal due to fracture is required in 3–18 % of mandibular reconstruction surgeries [2–6], and one of the major causes of these fractures is the residual stress in the plate that accumulates during repeated bending. Martola et al. reported that the adjustive bending of plates during surgical operations generates residual stress, eventually resulting in the fracture of the plate [7]. Using finite element (FE) analysis, we have also previously demonstrated that the residual stress in a plate generated during the bending process adversely affects plate stability [8]. It is thus crucial to bend the plate to the desired angle in a single trial to minimize the risk of plate fracture and the need for additional surgery.

In the bending procedure, spring-back occurs when the bending load is removed; as such, the final bent angle is lower than the input angle. To obtain the desired angle in a single trial, the input angle must be greater than the target angle to compensate for spring-back. However, there is no practical way to predict the input angle required because the degree of spring-back varies with the material, bending angle, and plate geometry [9–12]. Conventional trial-and-error methods are based on a table of empirical input and final bent angles for specific plates, but this method is time-consuming and expensive. Additionally, empirical rule-based adjustments for spring-back may not apply to complicated plate geometries [13, 14]. Various numerical approaches to estimating the amount of spring-back based on FE analysis have been reported

Table 1. Specification of the components used for the motorized bending apparatus.

Component	Model
Power supply	LRS-150F-24, Mean Well, Taiwan
Microcontroller	Arduino UNO, Arduino, Italy
Motor driver	MD5-HD14, Autonics, Korea
Geared stepper motor	A200K-599-G10, Autonics, Korea
Bending element	Clamp, clamp base, pusher plate, rotary knob

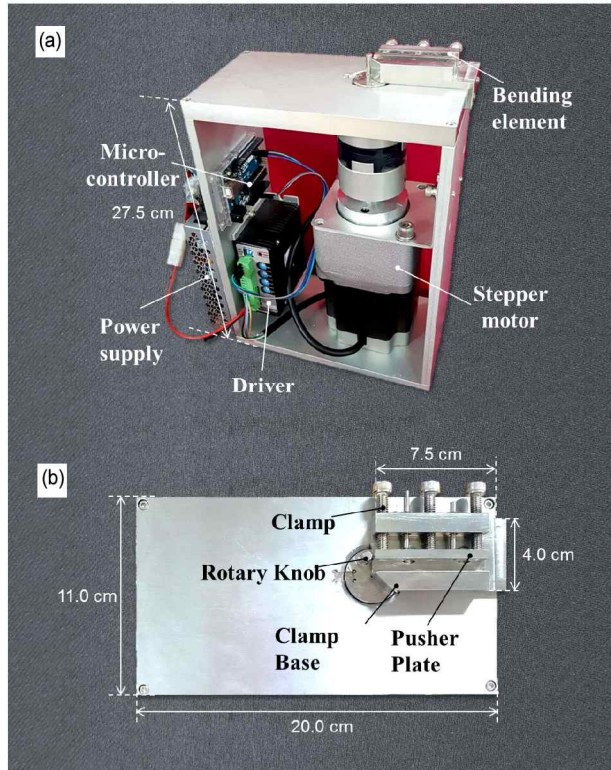


Fig. 1. The proposed motorized bending apparatus: (a) Overall appearance; (b) top view of the components of the bending element.

[15-18]; however, these cannot be directly used to calculate the required input angle to compensate for spring-back. Rather, they are frequently used to calculate the amount of spring-back for a given input angle.

In this paper, we propose an iterative FE procedure to calculate the input bending angle to achieve the desired bending angle after spring-back. This is based on a plate-bending procedure using a motorized bending apparatus that we developed in a previous study [19]. As shown in Fig. 1 and Table 1, the motorized bending apparatus consists of a power supply, microcontroller, motor driver, geared stepper motor, and bending element. In the bending process, a surgical plate is fixed by tightening the clamp of the bending element. The stepper motor is connected to the rotary knob so that the motor rotates the knob by the set input angle. After holding this position for 5 seconds, the rotary knob rotates back to the initial position, which is when spring-back occurs. Further details on the mo-

torized bending apparatus are provided in Ref. [19].

In the proposed bending-angle calculation, the optimal input angle is obtained using iterative FE analysis to predict the relationship between the input bending angle and the final bent angle after spring-back. To assess the performance of the proposed approach, experiments with two different target angles are conducted in the present study.

## 2. Material and method

### 2.1 Initial input-angle calculation based on geometric information

The bending angle  $\alpha$  is a function of the rotating angle of the knob  $\theta$ , the geometry  $\mathbf{G}$ , and the material properties  $\mathbf{M}$ :

$$\alpha = F(\theta, \mathbf{G}, \mathbf{M}). \quad (1)$$

In general, Eq. (1) is a complex nonlinear function with many specific variables due to the complex nature of  $\mathbf{G}$  and  $\mathbf{M}$ . To produce the desired bending angle  $\alpha_D$ , we need to satisfy

$$\alpha_D = F(\theta_D, \mathbf{G}_D, \mathbf{M}_D) = F_D, \quad (2)$$

where the input angle  $\theta_D$  for the desired bending angle  $\alpha_D$  is the solution variable to be calculated. Because the bending angle has a non-linear relationship with the input rotating angle, it is necessary to iterate the solution for Eq. (2). Because the desired bending angle  $\alpha_D$  is independent of the configuration of the plate or the rotation, the Newton-Raphson iteration for Eq. (2) becomes

$$\Delta F^{(i-1)} = \alpha_D - F_D^{(i-1)} \quad (3)$$

$$K_D^{(i-1)} \Delta \theta^{(i)} = \Delta F^{(i-1)} \quad (4)$$

$$\theta^{(i)} = \theta^{(i-1)} + \Delta \theta^{(i)} \quad (5)$$

with initial guesses  $\theta^{(0)} = \theta_0$  and  $F_D^{(0)} = \alpha_0$ , where the superscript  $(i)$  denotes the value for the  $i$ -th iteration,  $\Delta F$  is the increase in the bending angle,  $\Delta \theta$  is the increase in the input rotating angle, and  $K_D^{(i-1)}$  is the current tangent stiffness, leading to

$$K_D^{(i-1)} = \left. \frac{\partial F}{\partial \theta} \right|_{\theta^{(i-1)}}. \quad (6)$$

The iterations continue until the appropriate convergence criteria are satisfied.

A characteristic of this iteration process is that a new tangent stiffness is calculated with each iteration, which is computationally demanding. Moreover, it is not practically feasible to obtain the exact function  $F$  in Eq. (1) for a plate with general geometry and material properties; the widely used tables listing empirical values for Eq. (1) have been created only for plates with a specific geometry and material.

In this study, we use an approximated tangent stiffness:

$$K_D^{(i-1)} = \frac{\partial F}{\partial \theta} \bigg|_{\theta^{(i-1)}} \doteq \frac{\alpha^{(i-1)} - \alpha^{(i-2)}}{\theta^{(i-1)} - \theta^{(i-2)}}. \quad (7)$$

Based on Eqs. (3)-(5), the tangent stiffness in Eq. (7) results in the following simple improved solution:

$$\theta^{(i)} = \theta^{(i-1)} + \frac{\alpha^{(i-1)} - \alpha^{(i-2)}}{\theta^{(i-1)} - \theta^{(i-2)}} (\alpha_D - \alpha^{(i-1)}). \quad (8)$$

Note that, in this iterative process, any computational method can be used in the calculation of the solution at each iteration, and a plate with a generalized geometry and material properties can be considered. For example, as in the present study, at each iteration, commercial FE software can be used to calculate the bending angle after spring-back  $\alpha^{(i-1)}$  for the given input rotating angle  $\theta^{(i-1)}$  and to update the input rotating angle  $\theta^{(i)}$  with a simple user input code representing Eq. (8).

While the final converged solution depends on the accuracy of the solution for each iteration, it is crucial that the initial guesses are close to the final solution to reduce the number of iterations required and to ensure convergence. For the initial guess  $\theta_0$ , we use a solution that assumes no spring-back, which can be calculated from the geometrical relationship between the bending element in the developed bending apparatus and the plate. Assuming no spring-back, the input rotating angle  $\theta_A$  required to create plate bending angle  $\alpha_D$  is calculated based on the approximated shape of the bent plate shown in Fig. 2 as

$$\theta_A = \pi - \omega - \arcsin\left(\frac{r + s + t}{R}\right) + \alpha_D \quad (9)$$

For iteration  $i = 1$ , we approximate the tangent stiffness  $K_D^0$  as 1, assuming that the incremental amount of spring-back is the same as that of the input angle. The convergence criteria are met when  $i$  is greater than 50 or the difference between  $\alpha_D$  and  $\alpha^{(i)}$  is less than  $0.05^\circ$ . The step-by-step process for the iterative FE process is summarized in Table 2.

## 2.2 Bending-angle calculation using FE analysis

In this paper, the iterative calculations are conducted using Abaqus v.6.14 (Dassault Systèmes SIMULIA Corp., Providence, RI, USA) for the bending of the reconstruction plate (24-RS-015, JEIL Medical Corp., Korea) with the proposed motorized bending apparatus, consisting of two steps: (1) Loading the plate by rotating the knob and (2) removing the load by allowing the knob to return to its original position. Based on the bending conditions in practice, it is assumed that plate bending occurs for a duration of 5 seconds. The bending angles measured at each step are denoted by  $\alpha_{step1}$  (the bending angle before spring-back) and  $\alpha_{step2}$  (the bending angle after spring-back;  $\alpha^{(i)}$ ); the difference between these indicates the pre-

Table 2. Step-by-step solution.

```

IF  $i = 0$  THEN
     $\theta_i = \theta_A$ 
ELSE IF  $i = 1$  THEN
     $\theta_i = \theta_{i-1} + (\alpha_D - \alpha_i)$ 
ELSE
    DO
         $\theta_i = \theta_{i-1} + \frac{(\theta_{i-1} - \theta_{i-2})(\alpha_D - \alpha_{i-1})}{(\alpha_{i-1} - \alpha_{i-2})}$ 
    IF  $i \geq 50$  OR  $|\alpha_D - \alpha_i| < 0.05$  EXIT
     $i = i + 1$ 
    ENDDO
ENDIF

```

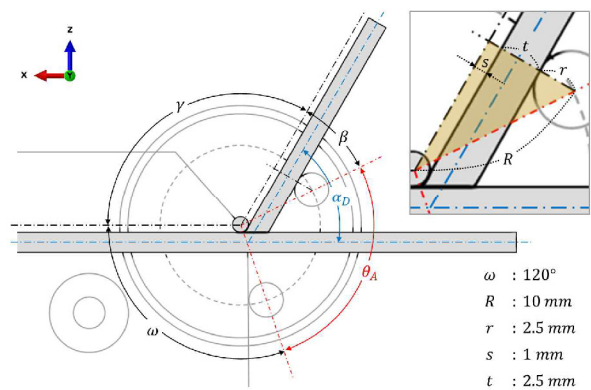


Fig. 2. The geometric relationship between the bending elements of the bending apparatus and the plate.

dicted spring-back ( $\alpha_{sp}$ ). As shown in Fig. 3, the components directly related to plate bending are analyzed: The clamp base, the rotary knob, and the reconstruction plate. The material properties assigned to each component are summarized in Table 3 [20, 21] assuming they are isotropic and homogeneous. Each part is divided into four-node tetrahedral structural elements; the total number of nodes and elements in each model is listed in Table 4. In particular, the bending region of the plate is set to a much denser mesh size than the other parts to ensure accurate analysis: 0.2 mm is selected based on a mesh convergence test considering the convergence of the spring-back angle and computer analysis time.

## 2.3 Experiments

Experiments are carried out for two target bending angles ( $15^\circ$  and  $30^\circ$ ). A total of 10 reconstruction plates that are identical to the model used in the angular calculation described above are used. Each plate has two bending regions: Between the sixth and seventh screw-holes on both sides, as shown in Fig. 4. The bending tests using the initial guess input angle ( $\theta_A$ ) and the calculated input angle ( $\theta_{FE}$ ) are conducted on each bending area and the results are compared. Each step is recorded with a camera perpendicular to the bending element



Table 3. Material properties [20, 21].

Material	Young's modulus [MPa]	Poisson ratio	Tensile yield stress [MPa]	Ultimate tensile stress [MPa]
SUS303*	193000	0.25	-	-
Titanium grade 3	116000	0.37	450	550

\*SUS303: Plate bender components

Table 4. The number of elements and nodes in the FE model.

Components	Element #	Node #
Clamp base	5616	1490
Rotary knob	5415	1263
Reconstruction plate	611627	106109

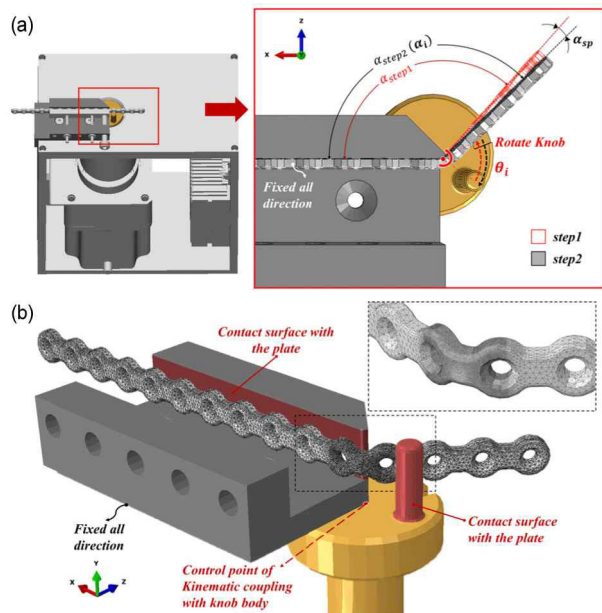


Fig. 3. Set-up of the finite element model: (a) The bent shape of the plate under loading (red line; step 1) and unloading (black line; step 2) after spring-back; (b) the red surfaces show the contact surfaces with the plate. The knob is rotated around a control point connected to the body, and the dotted box indicates the denser mesh size in the bent area.

of the bending apparatus and the resulting plate angle before and after spring-back is measured using the acquired images.

### 3. Results

Fig. 5 presents the plate deformation during the bending simulation for each step. As shown in Fig. 5(b), the residual stress remains after plastic deformation in the bending area of the plate. As mentioned in Sec. 2.2, if the difference between the desired angle ( $\alpha_D$ ) and the measured bent angle after spring-back ( $\alpha_{sp2}$ ) is more than 0.05°, the input angle ( $\theta$ ) is updated using the process outlined in Table 2.

The results of the iterative FE analysis are summarized in

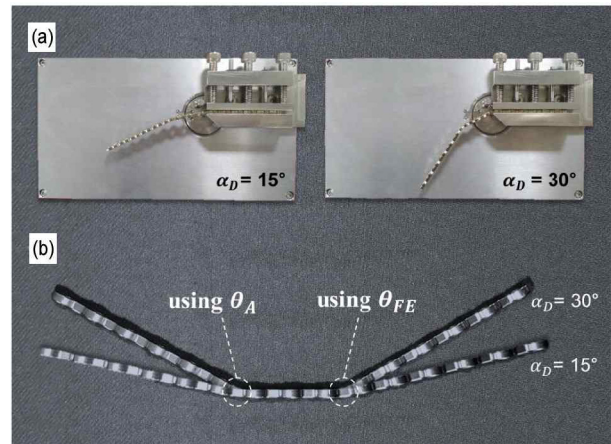


Fig. 4. (a) Experiments bending the plate by 15° and 30°; (b) bent regions (between the sixth and seventh screw hole from both ends of the plate).

Table 5. They show that  $\alpha_i$  converges to the target angle with repeated simulations. The simulation for  $\alpha_D = 15^\circ$  satisfies the ending condition (i.e., the difference between  $\alpha_D$  and  $\alpha_i$  is less than 0.05°) after the third iteration. Similarly, the simulation for  $\alpha_D = 30^\circ$  is completed after the second iteration. The final input angle in each case ( $\theta_{FE}$ ) is calculated using a spring-back angle of 3.29° and 3.64° when  $\alpha_D$  is 15° and 30°, respectively. When the target angles ( $\alpha_D$ ) are 15° and 30°, the error rates are 14.00 % and 2.53 %, respectively, using  $\theta_A$  as the initial guess. It is expected that the error rate could be reduced to 0.27 % and 0.03 %, respectively, when  $\theta_{FE}$  is used.

For the bending experiments, the average bending angle before and after spring-back is presented in Fig. 6. In the 15° bending test, the final bent angle obtained using the input angle  $\theta_A$  is 12.89° and the error is 14.06 %. The bent angle obtained using  $\theta_{FE}$  as the input angle is 15.02° and the error is reduced to 2.53 %. In the 30° bending test, the error rate decreases from 0.13 % to 0.07 % when using  $\theta_{FE}$  instead of  $\theta_A$ .

### 4. Discussion

A surgical plate used to repair a defective mandible must fit the surgical region well. The shape of the plate governs the stability of the reconstruction and facial appearance. To prevent plate fractures, two approaches have been taken to reduce the accumulation of stress in plates. One approach involves the design of customized plates and the other is related to developing bending methods to minimize the change in the mechanical properties of the plates.

Customized plates are advantageous in that they do not require intraoperative bending and offer higher accuracy compared to stock plates. However, their costs due to virtual planning exceed the costs of standard plates [22]. Additionally, depending on the design of the custom plate, the results of the surgery can vary [23-26], so additional research is needed to establish a method to improve the design. Therefore, in the present study, we focus on developing a bending method that

Table 5. Results of the simulations for bending-angle calculations.

$\alpha_D$	15°					30°				
$i$	$\alpha_{step1}$	$\alpha_{step2}(\alpha_i)$	$\alpha_{sp}$	$ \alpha_D - \alpha_i $	$\theta_i$	$\alpha_{step1}$	$\alpha_{step2}(\alpha_i)$	$\alpha_{sp}$	$ \alpha_D - \alpha_i $	$\theta_i$
0	16.15°	12.90°	3.25°	2.10	38.13°	32.87°	29.24°	3.63°	0.76	53.13°
1	18.42°	15.13°	3.29°	0.13	40.23°	33.74°	30.10°	3.64°	0.10	53.89°
2	18.29°	14.93°	3.36°	0.07	40.10°	33.65°	30.01°	3.64°	0.01	53.80°
3	18.33°	15.04°	3.29°	0.04	40.15°	-	-	-	-	-

$\alpha_D$  : Desired angle,  $\alpha_{step1}$  : Bending angle after loading (before spring-back),  $\alpha_{step2}$  : Bending angle after unloading (after spring-back),  $\alpha_{sp}$  : Amount of spring-back predicted,  $\theta_i$  : i-th input angle calculated,  $i$  : Iteration number

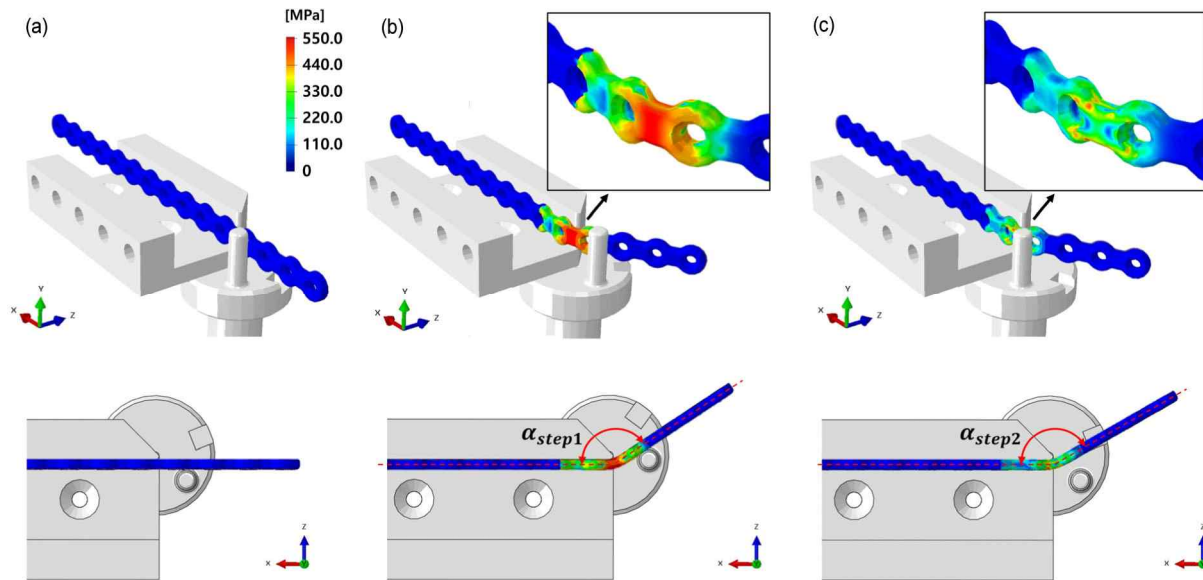


Fig. 5. Deformation and von Mises stress distributions within the plate during the bending simulation: (a) Initial state before applying the bending load; (b) during the application of the bending load using the knob (step 1); (c) after spring-back following the removal of the bending load (step 2).

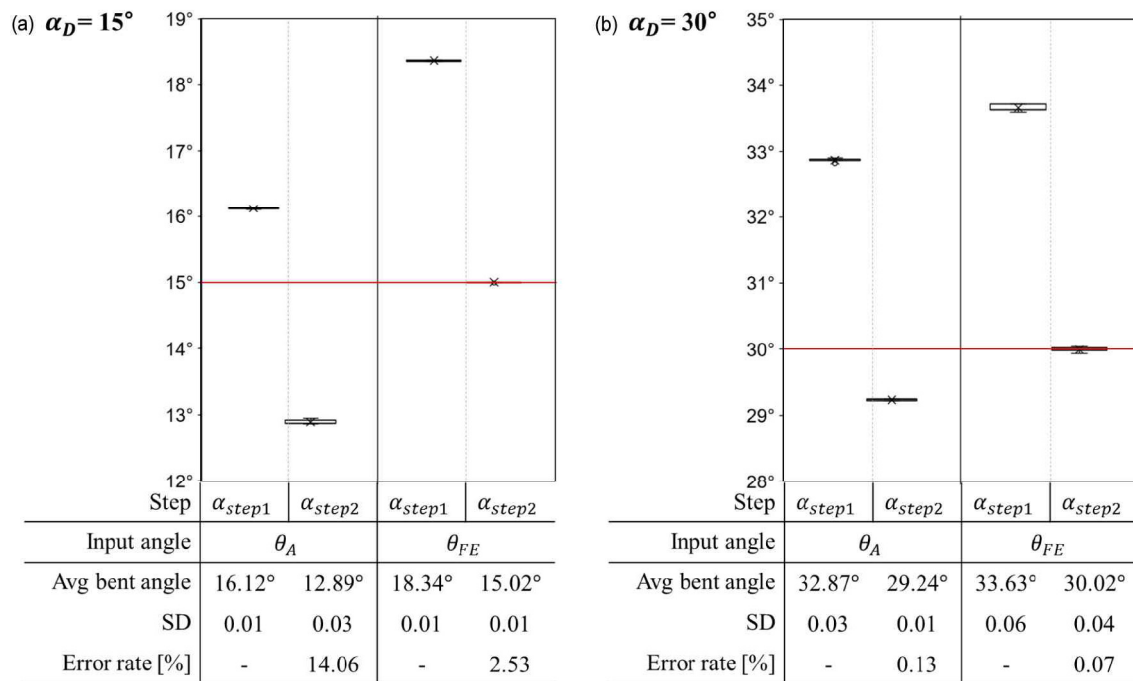
considers the biomechanical stability of conventional plates.

Several studies have conducted FE simulations of the surgical plate-bending process. For example, Harith et al. investigated the optimal shape for tibial plates required for optimal fit within a given dataset and investigated whether they could be obtained by manually deforming a conventional plate [27]. The bending methods assumed that current bending tools were used to obtain the desired plate shape, and the safety factor of the resultant plate was calculated to determine whether it was viable for tibial reconstruction. Although it can be used to produce an optimal shape with existing tools, this process had to be repeated many times because the spring-back of the plate was not considered in the bending process. Ridwan-Pramana et al. used calculated stiffness values for a fixing plate subject to tension, torsion, bending, and shear processes to investigate the effect of the shape and the bone-implant interface on the stress distribution within skull implants [28]. Although segmented bending processes were considered, their study did not consider the number of repetitions required in the bending process.

In the present study, we develop a new bending apparatus that improves upon three limitations of the current manual bending process [19]. The first limitation is the inconvenience of current bending equipment such as the bending press and bending irons. Because conventional bending equipment is operated manually, the physical force depends on the surgeon's experience. In particular, when bending a thick plate, manipulation is often difficult because it requires a lot of force.

Another limitation is the time-consuming nature of the bending process. According to manual bending tests conducted by Clijmans et al., an operator needed about 26 minutes to bend a 2.4-mm uni-lock reconstruction plate to fit a synthetic mandible model [29]. The manual bending process is performed repeatedly to bend the plate accurately at the desired angle. Because this repetitive bending is usually performed during surgery, the increase in operating time directly leads to an increase in operating room costs. According to Toto et al., even though additional pre-operative costs would be incurred, establishing a meticulous surgery plan helps to reduce the total cost of surgery [30].

## The results of the bending experiments



\*  $\alpha_D$ : desired bending angle,  $\theta_A$ : input angle assuming no spring-back,  $\theta_{FE}$ : input angle obtained by the FE simulations,  $\alpha_{step1}$ : the bent angle before spring-back,  $\alpha_{step2}$ : the bent angle after spring-back, Avg : average, SD : Standard deviation

Fig. 6. The results of the bending experiments when (a)  $\alpha_D = 15^\circ$ ; (b)  $\alpha_D = 30^\circ$ .

The third issue is the biomechanical stability of the bent plate and its role in plate fractures. Fatigue and changes in the mechanical properties within a plate due to the repeated bending of the plate can create micro-cracks that can lead to plate failure after surgery [7, 31-34]. Therefore, it is necessary to minimize the plastic deformation process of the plate to reduce cumulative stress and changes in the mechanical characteristics within the plate.

We thus propose a new bending apparatus to overcome the challenges associated with conventional manual bending, including the inconvenience of existing tools, the requirement of great physical strength to bend thick plates, inconsistent bending results, and prolonged operating times. We can also predict the plate spring-back angle using FE simulations to produce the desired angle with a single bend. Because automatic equipment is used, it is much easier to obtain accurate results without operator variation. Furthermore, accurate results can be achieved in less time. The spring-back predictions using the proposed process agree well with bending experiments designed to determine whether the process leads to an improvement in terms of accuracy. One limitation of the present study is that it only considers bending with respect to one point along one axis. Future research is required to consider a more generalized bending process that incorporates various bending axes and points. Also, further studies should include a strain-stress curve for different strain rates.

## 5. Conclusions

In this paper, we introduced a surgical plate bending process with an automated bending apparatus that can replace repetitive manual bending with conventional bending equipment. Using the proposed process, bending angles to be used as input to the apparatus were calculated considering the predicted spring-back. The results of the experiments testing the effect of the input angle in the proposed bending apparatus revealed that the predicted angle of spring-back was very similar to the measured angle and that the accuracy of the bending angle for the plate was greatly improved. In addition, because the bending tests using the proposed apparatus required only a single bend, the concentration of the residual stress within the bent area would be lower than for repetitive manual bending. The higher accuracy of the plate shape and the simplified bending process offer significant advantages for reconstructive surgery, such as reduced operating times, increased convenience, and improved plate stability.

## Acknowledgments

This work was supported by the KIST Institutional Program (2E29330) and by a grant from the Korea Health Technology R&D Project through the Korea Health Industry Development Institute (KHIDI), funded by the Ministry of Health & Welfare,

Republic of Korea (H18C1224).

## Nomenclature

$R$	: Radius of the rotary knob
$r$	: Radius of the knob directly in contact with the plate
$s$	: Radius of the center point of the rotary knob
$t$	: Thickness of the plate
$\alpha_D$	: Desired bending angle
$\alpha_i$	: The bent angle after spring-back of the plate for the $i$ -th iteration
$\alpha_{step1}$	: The bent angle before spring-back in a plate
$\alpha_{step2}$	: The bent angle after spring-back in a plate
$\beta$	: Angle between the center of the knob and the bent plate
$\gamma$	: Angle between the bent plate and clamp base
$\omega$	: Angle indicating the position of the initial knob relative to the clamp base
$i$	: The number of iterations
$\theta_A$	: Input angle to rotate the knob from the initial position, related to geometric approximate expressions
$\theta_{FE}$	: Input angle to rotate the knob from the initial position, calculated using finite element analysis
$\theta_i$	: Input angle entered for the $i$ -th iteration

## References

- [1] S.-M. Park, J.-W. Lee and G. Noh, Which plate results in better stability after segmental mandibular resection and fibula free flap reconstruction?: Biomechanical analysis, *Oral Surgery, Oral Medicine, Oral Pathology, and Oral Radiology*, 126 (5) (2018) 380-389.
- [2] R. Lopez, C. Dekeister, Z. Sleiman and J. R. Paoli, Mandibular reconstruction using the titanium functionally dynamic bridging plate system: A retrospective study of 34 cases, *Journal of Oral and Maxillofacial Surgery*, 62 (4) (2004) 421-426.
- [3] P. Maurer, A. W. Eckert, M. S. Kriwalsky and J. Schubert, Scope and limitations of methods of mandibular reconstruction: A long-term follow-up, *British Journal of Oral and Maxillofacial Surgery*, 48 (2) (2010) 100-104.
- [4] T. Shibahara, H. Noma, Y. Furuya and R. Takaki, Fracture of mandibular reconstruction plates used after tumor resection, *Journal of Oral and Maxillofacial Surgery*, 60 (2) (2002) 182-185.
- [5] A. Sakakibara, K. Hashikawa, S. Yokoo, S. Sakakibara, T. Komori and S. Tahara, Risk factors and surgical refinements of postresective mandibular reconstruction: A retrospective study, *Plastic Surgery International* (2014).
- [6] G. J. Seol, E. G. Jeon, J. S. Lee, S. Y. Choi, J. W. Kim, T. G. Kwon and J. Y. Paeng, Reconstruction plates used in the surgery for mandibular discontinuity defect, *Journal of the Korean Association of Oral and Maxillofacial Surgery*, 40 (6) (2014) 266-271.
- [7] M. Martola, C. Lindqvist, H. Hänninen and J. Al-Sukhun, Fracture of titanium plates used for mandibular reconstruction following ablative tumor surgery, *Journal of Biomedical Materials Research Part B Applied Biomaterials*, 80 (2) (2007) 345-352.
- [8] S. M. Park, D. Lee, J. W. Lee, Y. Kim, L. Kim and G. Noh, Stability of the permanently bent plates used in mandibular reconstructive surgery, *EMBC, IEEE 38th Annual International Conference* (2016) 2198-2201.
- [9] D. W. Jung, A parametric study of sheet metal denting using a simplified design approach, *KSME International Journal*, 16 (12) (2002) 1673-1686.
- [10] D. K. Leu and Z. W. Zhuang, Springback prediction of the vee bending process for high-strength steel sheets, *Journal of Mechanical Science and Technology*, 30 (3) (2016) 1077-1084.
- [11] A. Ktari, Z. Antar, N. Haddar and K. Elleuch, Modeling and computation of the three-roller bending process of steel sheets, *Journal of Mechanical Science and Technology*, 26 (1) (2012) 123-128.
- [12] K. A. Al-Ghamdi, Spring back analysis in incremental forming of polypropylene sheet: An experimental study, *Journal of Mechanical Science and Technology*, 32 (10) (2018) 4859-4869.
- [13] H. S. Lee, J. H. Kim, G. S. Kang, D. C. Ko and B. M. Kim, Development of seat side frame by sheet forming of DP980 with die compensation, *International Journal of Precision Engineering and Manufacturing*, 18 (1) (2017) 115-120.
- [14] B. S. Levy, Empirically derived equations for predicting springback in bending, *Journal of Applied Metalworking*, 3 (2) (1984) 135-141.
- [15] N. Montmayeur and C. Staub, Springback prediction with OPTRIS, *Proc. of NUMISHEET* (1999) 41-46.
- [16] K. Kazama, T. Nukaga and H. Makino, Springback simulation of truck's frame side member, *Proc. of NUMISHEET* (1999) 65-70.
- [17] U. Abdelsalam, A. Sikorshi and M. Karima, Application of one step springback for product and early process feasibility of sheet metal stampings, *In NUMISHEET*, 99 (1999) 47-52.
- [18] M. S. Lee, H. Y. Seo and C. G. Kang, Comparative study on drawability of CR340/CFRP composites by using theoretical and experimental methods, *Journal of Precision and Engineering and Manufacturing-Green Technology*, 4 (1) (2017) 97-104.
- [19] S. Park, J. Lee, S. M. Park, G. Noh, J. W. Lee, M. S. Park and Y. Kim, A novel motorized bending apparatus for surgical plates, *Journal of Mechanical Science and Technology*, 33 (8) (2019) 3743-3748.
- [20] P. D. Harvey, *Engineering Properties of Steels*, American Society for Metals, Metals Park, OH (1982).
- [21] R. Boyer, G. Welsch and E. W. Collings, *Materials Properties Handbook: Titanium Alloys Eds.*, ASM International, Materials Park, OH (1994).
- [22] R. Gutwald, R. Jaeger and F. M. Lambers, Customized mandibular reconstruction plates improve mechanical performance in a mandibular reconstruction model, *Computer Methods in Biomechanics and Biomedical Engineering*, 20 (4) (2017) 426-435.
- [23] D. Luo, X. Xu, C. Guo and Q. Rong, Fracture prediction for a customized mandibular reconstruction plate with finite element method, *LSMS 2017, Communications in Computer and Information Science*, 761 (2017) 86-94.
- [24] M. Kozakiewicz and J. Swiniarski, "A" shape plate for open rigid internal fixation of mandible condyle neck fracture, *Journal*



of *Cranio-Maxillofacial Surgery*, 42 (6) (2014) 730-737.

- [25] N. Narra, J. Valášek, M. Hannula, P. Marcián, G. K. Sándor, J. Hyttinen and J. Wolff, Finite element analysis of customized reconstruction plates for mandibular continuity defect therapy, *Journal of Biomechanics*, 47 (1) (2014) 264-268.
- [26] P. Li, L. Shen, J. Li, R. Liang, W. Tian and W. Tang, Optimal design of an individual endoprosthesis for the reconstruction of extensive mandibular defects with finite element analysis, *Journal of Cranio-Maxillofacial Surgery*, 42 (1) (2014) 73-78.
- [27] H. Harith, B. Schmutz, J. Malekani, M. A. Schuetz and P. K. Yarlagadda, Can we safely deform a plate to fit every bone? Population-based fit assessment and finite element deformation of a distal tibial plate, *Medical Engineering & Physics*, 38 (3) (2016) 280-285.
- [28] A. Ridwan-Pramana, P. Marcián, L. Borák, N. Narra, T. Forouzanfar and J. Wolff, Structural and mechanical implications of PMMA implant shape and interface geometry in cranioplasty – A finite element study, *Journal of Cranio-Maxillofacial Surgery*, 44 (1) (2016) 34-44.
- [29] T. Clijmans, J. Abeloos, P. Lamoral, C. De Clercq, G. Wouters, P. Suetens and J. Vander Sloten, Mandibular reconstruction plate bending: Time and accuracy, *Journal of Cranio-Maxillofacial Surgery*, 36 (2008) S82.
- [30] J. M. Toto, E. I. Chang, R. Agag, K. Devarajan, S. A. Patel and N. S. Topham, Improved operative efficiency of free fibula flap mandible reconstruction with patient - Specific, computer-guided preoperative planning, *Head & Neck*, 37 (2015) 1660-1664.
- [31] J. M. Doty, D. Pienkowski, M. Goltz, R. H. Haug, J. Valentino and O. A. Arosarena, Biomechanical evaluation of fixation techniques for bridging segmental mandibular defects, *Archives of Otolaryngology-Head & Neck Surgery*, 130 (12) (2004) 1388-1392.
- [32] W. D. Knoll, A. Gaida and P. Maurer, Analysis of mechanical stress in reconstruction plates for bridging mandibular angle defects, *Journal of Cranio-Maxillofacial Surgery*, 34 (4) (2006) 201-209.
- [33] T. Nagasao, J. Miyamoto, T. Tamaki and H. Kawana, A comparison of stresses in implantation for grafted and plate-and-screw mandible reconstruction, *Oral Surgery, Oral Medicine, Oral Pathology, and Oral Radiology*, 109 (3) (2010) 346-356.
- [34] C. Rendenbach, K. Sellenschloh, L. Gerbig, M. M. Morlock, B. Beck-Broichsitter, R. Smeets and H. Hanken, CAD-CAM plates versus conventional fixation plates for primary mandibular reconstruction: A biomechanical in vitro analysis, *Journal of Cranio-Maxillofacial Surgery*, 45 (11) (2017) 1878-1883.



**Si-Myung Park** is a Research Assistant in the Center for Medical Robotics at the Korea Institute of Science Technology. She received a B.S. degree in IT Engineering from Sookmyung Women's University (2016), and a M.S. degree in Mechanical Engineering from Yonsei University (2019). Her research interests include computational mechanics, biomechanics, and design optimization of structures.



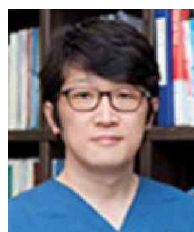
**Jeonghwan Lee** is a Ph.D. student in the Walker Department of Mechanical Engineering, the University of Texas at Austin. He received a B.S. degree in Mechanical Engineering from Hanyang University in 2013, and a M.S. degree in Mechanical and Aerospace Engineering from Seoul National University in 2017.

He was a research assistant in the Center for Bionics at Korea Institute of Science Technology in 2017. His research interests include robotics and rehabilitation engineering.



**Seungbin Park** is a M.S. student in the Department of Computer Science and Engineering, Korea University and a research assistant in the Center for Bionics at the Korea Institute of Science Technology. She received a B.S. degree in the Department of Biomedical Engineering, Yonsei University (2018). Her research interests include deep learning in the medical field and medical image processing.

Her research interests include deep learning in the medical field and medical image processing.



**Jung-Woo Lee** is an Associate Professor in the Department of Oral and Maxillofacial Surgery at the School of Dentistry, Kyung Hee University Dental Hospital. He received his D.M.D. (2003), M.S.D. (2006), and Ph.D. (2011) from the School of Dentistry at Kyung Hee University. His research interests include virtual surgical simulation and 3D bioprinted tissue regeneration.

simulation and 3D bioprinted tissue regeneration.



**Min Soo Park** is an Associate Professor in the Department of Mechanical System Design Engineering, Seoul National University of Science and Technology. He received his B.S. (2001) and Ph.D. (2007) from the School of Mechanical and Aerospace Engineering at Seoul National University. His research interests are metal and ceramic 3D printing, laser processing, and micro-machining.

His research interests are metal and ceramic 3D printing, laser processing, and micro-machining.



**Youngjun Kim** is a Principal Researcher in the Center for Bionics at Korea Institute of Science Technology. He received his B.S. (2001), M.S. (2003), and Ph.D. (2009) in the School of Mechanical and Aerospace Engineering at Seoul National University. He researched in the Department of Radiation Oncology at Stanford University as a postdoctoral scholar (2013). His research interests include 3D medical software, computer aided design, and deep learning for medicine.

His research interests include 3D medical software, computer aided design, and deep learning for medicine.





**Gunwoo Noh** is an Assistant Professor in the School of Mechanical Engineering, Kyungpook National University. He received a B.S. degree in Mechanical Engineering from the Korea Advanced Institute of Science and Technology, Daejeon, Korea in 2009, and M.S. and Ph.D. degrees in Mechanical Engineering from

Massachusetts Institute of Technology, Cambridge, MA, USA in 2011 and 2013, respectively. His research interests include computational mechanics, structural dynamics, numerical integrations, biomechanics, and the design optimization of structures.